Michal Beneš; Petr Mayer

Numerical analysis of mathematical model of heat and moisture transport in concrete at high temperatures

In: Jan Chleboun and Karel Segeth and Tomáš Vejchodský (eds.): Programs and Algorithms of Numerical Mathematics, Proceedings of Seminar. Prague, May 28-31, 2006. Institute of Mathematics AS CR, Prague, 2006. pp. 16–23.

Persistent URL: http://dml.cz/dmlcz/702813

NUMERICAL ANALYSIS OF MATHEMATICAL MODEL OF HEAT AND MOISTURE TRANSPORT IN CONCRETE AT HIGH TEMPERATURES*

Michal Beneš, Petr Mayer

Abstract

In this paper, we present a nonlinear mathematical model for numerical analysis of the behaviour of concrete subject to transient heating according to the standard ISO fire curve. This example allows us to analyse and better understand physical phenomena taking place in heated concrete (thermal spalling).

1. Balance equations of mathematical model

The behaviour of concrete at high temperature is dependent on its composite structure, on the physical and chemical composition of the cement paste, which is a highly porous, hygroscopic material. In the whole temperature range, the gas phase is a mixture of dry air and water vapour. Therefore, the moist concrete is modelled as a multiphase material.

The global multiphase system is treated within the framework of averaging theories starting from microscopic level and applying mass, area and volume averaging operators to the local form of governing equations.

The mathematical model consists of the following balance equations for the α-phase, in particular w, resp. g, resp. ga, resp. gw denotes the liquid phase, resp. the gas phase, resp. the dry air, resp. water vapour,

$$\frac{D^\alpha}{Dt}(\eta^\alpha\rho^\alpha) + (\eta^\alpha\rho^\alpha)\nabla\cdot\mathbf{v}^\alpha = \hat{e}^\alpha_\beta, \quad \alpha,\beta = w,\, gw,\, ga, \quad \alpha\neq\beta, \tag{1}$$

$$(\rho C)\frac{\partial T}{\partial t} + (\rho C\mathbf{v})\nabla\cdot T - \nabla\cdot(\lambda\nabla T) = -\dot{m}_{phase}\Delta h_{phase} + \dot{m}_{dehydr}\Delta h_{dehydr}, \tag{2}$$

where η^α is the volume fraction of phase α,

$$\eta_w = \phi S_w, \quad \eta_g = \phi S_g, \quad S_w + S_g = 1,$$

where S_w, resp. S_g denotes the degree of water saturation, resp. the degree of gas saturation, ϕ is the porosity, ρ^α and $\mathbf{v}^\alpha$ denote the averaged density and mass-averaged velocity of the α-phase. The mass source term $\hat{e}^\alpha_\beta$ on the right-hand side represents

*This research has been supported by Ministry of Education, Youth and Sports of the Czech Republic, No. 1M6840770001 within the frame of research centre CIDEAS and VZ 03 CEZ MSM 6840770003.

exchange of mass with interfaces separating individual phases (phase changes), as well as the terms on the right hand side of (2) represent the energy required for evaporation of liquid water and the energy required for release of bound water by dehydration. The convection term $(\rho C\mathbf{v})\nabla \cdot T$ in equation (2) is ignored provided that the transfer of energy by convection is included in the empirical relationship for the thermal conductivity $\lambda = \lambda(T)$.

2. Boundary and initial conditions

The model consisted of a rectangular section of the concrete wall, 0.1 m thickness, exposed to transient heating from one side according to the standard ISO FIRE curve

$$T_\infty(t) = T_{ISO-FIRE}(t) = 345\log(8t+1) + 293.15, \quad [t] = \text{min}. \tag{3}$$

In the case of heat transfer through the boundary at normal temperatures, the boundary conditions correspond to the Newton's law of cooling (Neuman's conditions)

$$-(\rho_w \mathbf{v}_l \Delta h_{phase} - \lambda \nabla T).\mathbf{n} = 0, \tag{4}$$

$$-(\rho_{gw}\mathbf{v}_g + \rho_w \mathbf{v}_l + \rho_g \mathbf{v}^d_{gw}).\mathbf{n} = 0. \tag{5}$$

On the part of the boundary, where the high temperature is analyse, the radiative boundary conditions

$$(\rho_w \mathbf{v}_l \Delta h_{phase} - \lambda \nabla T).\mathbf{n} = \alpha_c(T - T_\infty) + e\sigma(T^4 - T^4_\infty), \tag{6}$$

$$(\rho_{gw}\mathbf{v}_g + \rho_w \mathbf{v}_l + \rho_g \mathbf{v}^d_{gw}).\mathbf{n} = \beta_c(\rho_{gw} - \rho_{gw\infty}), \tag{7}$$

are of importance, where the terms on the right hand side of (6) represent the heat energy dissipated by convection and radiation to the surrounding medium, and the term on the ride hand side of (7) is the substance dissipated into the surrounding medium.

The initial conditions for concrete were set as follows: the uniform temperature $T = 293.15$ K, the uniform gas pressure 101325 Pa and the uniform capillary pressure 97.3 MPa, according to ρ_{gw} and ρ_{ga}.

3. Thermodynamic approach, constitutive relationships and material data

Dry air, water vapour and their mixture are assumed to behave as perfect gases, therefore Dalton's law and the Clapeyron equation are assumed as state equations. Water vapour pressure, p_{gw} is obtained from the Kelvin equation. As the constitutive equations for fluid phases (capillary water, gas phase) the multiphase Darcy's law has been applied.

Mathematical model of multiphase flow and heat transfer in concrete contains a several parameters and coefficients describing the properties of concrete and fluids: porosity $\phi = \phi(T)$, saturation $S = S(p_c)$, solid phase density $\rho = \rho(T)$, absolute permeability $\mathbf{K} = \mathbf{K}(p_g, T)$, relative permeability of gas phase $K_{rg} = K_{rg}(p_c, T)$, relative permeability of liquid phase $K_{rw} = K_{rw}(p_c, T)$, gas-phase dynamic viscosity $\mu_g = \mu_g(p_g, p_c, T)$, liquid phase dynamic viscosity $\mu_w = \mu_w(T)$, thermal capacity of the system $\rho C_p(T)$, thermal conductivity of the system $\lambda(T)$, enthalpy of vaporisation $\Delta h_{vap}(T)$. Formulas are given in detail in [3].

The relationship between capillary pressure and saturation in multiphase flow problems demonstrates memory effects and hysteresis. Differential equations with hysteresis have been the subject of studies, from the mathematical point of view, since 1960s. Hassanizadeh and Gray employ conservation laws for mass, momentum and energy, and the second law of thermodynamics in order to develop constitutive equations which describe two-phase flow in a porous medium (see [1], [2]). The following combination of terms contributes to the entropy production Λ:

$$T\Lambda = \ldots - \phi \dot{S}^w (p^g - p^w - p^c) + \ldots \geq 0.$$

For a linear theory, Hassanizadeh and Gray have suggested the relationship

$$p^g - p^w - p^c(S) + \tau(S)\dot{S} = 0,$$

where p^w, resp. p^g, designate the water, resp. the gas, pressure.

Under equilibrium condition without dynamic effects in the capillary relation the following definition of the capillary pressure can be used

$$p^c = p^g - p^w, \quad S_w = S_w(p^c). \tag{8}$$

In some particular cases, it is possible to use relation (8) even if the material system demonstrates hysteresis. For instance, in slow processes with monotonically decreasing (or increasing) saturation. Equation (8) is usually determined from experiments. In the literature several approximations of the relationship (8) have been suggested. In the present model the relationship

$$S_w(p_c) = S_r^w + (S_s^w - S_r^w)\left[1 + \left(\frac{p_c}{p_b^c}\right)^n\right]^{-m} \tag{9}$$

is employed. In (9) p_b^c denotes the air entry value, also referred to as bubbling pressure, which can be viewed as a characteristic pressure that has to be reached before the air actually enters the pores; m and n are empirical constants to fit the curves to experimental data.

A further step of this research is the influence of the dynamic or non-equilibrium effects and hysteresis, e.g. $\dot{S} \neq 0$, to hydro-thermal behavior of rapidly heated concrete.

4. Numerical algorithm

The space discretization of the energy conservation equation (2) is carried out by means of the finite element method ($h = 0.001$ m), we obtain the finite element model in the form

$$\mathbf{C}(\mathbf{T})\dot{\mathbf{T}} - \mathbf{K}(\mathbf{T})\mathbf{T} = \mathbf{f}(\mathbf{T}, \rho_{gw}, \rho_{ga}). \tag{10}$$

Time discretization of (10) is accomplished through an implicit difference scheme compared with $\mathbf{T}$ ($\Delta t = 1$ s)

$$[\mathbf{C}(\mathbf{T}_{n+1}) + \Delta t\mathbf{K}(\mathbf{T}_{n+1})]\,\mathbf{T}_{n+1} = \mathbf{C}(\mathbf{T}_{n+1})\mathbf{T}_n + \mathbf{f}(\mathbf{T}_{n+1}, \rho_{gw(n)}, \rho_{ga(n)}). \tag{11}$$

The Newton-Raphson method is applied to the nonlinear system (11) in the following iteration procedure: Let us denote

$$\Phi(\mathbf{T}^{(l)}_{n+1}) = \left[C_{ij}(\mathbf{T}^{(l)}_{n+1}) + \Delta t K_{ij}(\mathbf{T}^{(l)}_{n+1})\right]\mathbf{T}_{n+1} - C_{ij}(\mathbf{T}^{(l)}_{n+1})\mathbf{T}_n + f_i(\mathbf{T}^{(l)}_{n+1}, \rho_{gw(n)}, \rho_{ga(n)}),$$

then the solution at the end of the $(l+1)$st iteration is then given by

$$\mathbf{T}^{(l+1)}_{n+1} = \mathbf{T}^{(l)}_{n+1} - \mathbf{J}^{-1}_{\Phi}(\mathbf{T}^{(l)}_{n+1})\Phi(\mathbf{T}^{(l)}_{n+1}), \tag{12}$$

where $\mathbf{J}_\Phi$ is the (three-diagonal) Jacobi matrix.

Now we modify the dry air conservation equation and the water species conservation equation to the form

$$\begin{aligned}\phi\frac{\partial}{\partial t}\left[(1-S)\rho_{ga}\right] + (1-S)\rho_{ga}\frac{\partial\phi_{hydr}}{\partial t} + \nabla.(\rho_{ga}\mathbf{v}_g) + \nabla.(\rho_g\mathbf{v}^d_{ga}) &= 0, \qquad (13)\\ \phi\frac{\partial}{\partial t}\left[(1-S)\rho_{gw}\right] + (1-S)\rho_{gw}\frac{\partial\phi_{hydr}}{\partial t} + \nabla.(\rho_{gw}\mathbf{v}_g) + \nabla.(\rho_g\mathbf{v}^d_{ga}) &= \\ -\phi\frac{\partial}{\partial t}(S\rho_w) - S\rho_w\frac{\partial\phi_{hydr}}{\partial t} - \nabla.(\rho_w\mathbf{v}_l) - \frac{\partial}{\partial t}(\Delta m_{hydr}) & \qquad (14)\end{aligned}$$

with regard to Dalton's law and Clapeyron equations of state of perfect gases $\rho_g = \rho_{gw} + \rho_{ga}$ to the form

$$\phi\frac{\partial}{\partial t}\left[(1-S)\rho_{ga}\right] + (1-S)\rho_{ga}\frac{\partial\phi_{hydr}}{\partial t} + \nabla.(\phi(1-S)\rho_{ga}\mathbf{v}_g) + \nabla.(\phi(1-S)\rho_g\mathbf{v}^d_{ga}) = 0, \tag{15}$$

$$\begin{aligned}&\phi\frac{\partial}{\partial t}\left[(1-S)\rho_g + S\rho_w\right] + \left[(1-S)\rho_g + S\rho_w\right]\frac{\partial\phi_{hydr}}{\partial t} + \\ &+\nabla.(\phi\left[(1-S)\rho_g + S\rho_w\right]\mathbf{v}_g) + \nabla.(\phi S\rho_w(\mathbf{v}_w - \mathbf{v}_g)) = -\frac{\partial}{\partial t}(\Delta m_{hydr}). \qquad (16)\end{aligned}$$

Now we introduce the substitution $\mathbf{X} = (1-S)\rho_g + S\rho_w$, $\mathbf{Y} = (1-S)\rho_{ga}$ to (15) and (16)

$$\begin{aligned}\phi\frac{\partial\mathbf{Y}}{\partial t} + \mathbf{Y}\frac{\partial\phi_{hydr}}{\partial t} + \nabla.(\phi\mathbf{Y}\mathbf{v}_g) + \nabla.(\phi(1-S)\rho_g\mathbf{v}^d_{ga}) &= 0, \qquad (17)\\ \phi\frac{\partial\mathbf{X}}{\partial t} + \mathbf{X}\frac{\partial\phi_{hydr}}{\partial t} + \nabla.(\phi\mathbf{X}\mathbf{v}_g) + \nabla.(\phi S\rho_w(\mathbf{v}_w - \mathbf{v}_g)) &= -\frac{\partial}{\partial t}(\Delta m_{hydr}). \qquad (18)\end{aligned}$$

After discretization of the latter equaitons we get

$$X^j_i.\left[\phi^j_i - \Delta t_1\frac{A_h}{\rho_s}\frac{(T^n_i - T^{n-1}_i)}{\Delta t} + \Delta t_1\frac{\phi^j_i(v_g)^{j-1}_i}{h}\right] =$$

$$= \phi_i^j X_i^{j-1} + \Delta t_1 \frac{X_{i-1}^j (v_g)_{i-1}^{j-1} \phi_{i-1}^j}{h} - \Delta t_1 A_h \frac{T_i^n - T_i^{n-1}}{\Delta t} -$$

$$-\Delta t_1 \frac{\phi_i^j S_i^{j-1} (\rho_w)_i^j (v_w - v_g)_i^{j-1} - \phi_{i-1}^j S_{i-1}^{j-1} (\rho_w)_{i-1}^j (v_w - v_g)_{i-1}^{j-1}}{h}, \tag{19}$$

$$Y_i^j \cdot \left[\phi_i^j - \Delta t_1 \frac{A_h}{\rho_s} \frac{(T_i^n - T_i^{n-1})}{\Delta t} + \Delta t_1 \frac{\phi_i^j (v_g)_i^{j-1}}{h}\right] = \phi_i^j Y_i^{j-1} + \Delta t_1 \frac{Y_{i-1}^j (v_g)_{i-1}^{j-1} \phi_{i-1}^j}{h} +$$

$$+\Delta t_1 \frac{\phi_i^j (1 - S_i^{j-1}) (\rho_g)_i^j (v_{ga}^d)_i^{j-1} - \phi_{i-1}^j (1 - S_{i-1}^{j-1}) (\rho_g)_{i-1}^j (v_{ga}^d)_{i-1}^{j-1}}{h}, \tag{20}$$

where

$$\begin{aligned} X_i^j &= (1 - S_i^j)(\rho_g)_i^j + S_i^j (\rho_w)_i^j, \\ Y_i^j &= (1 - S_i^j)(\rho_{ga})_i^j. \end{aligned}$$

Since $\rho_g = \rho_{gw} + \rho_{ga}$, then

$$X_i^j = (1 - S_i^j)(\rho_{gw})_i^j + S_i^j (\rho_w)_i^j + Y_i^j. \tag{21}$$

Let us denote $\mathcal{F}((\rho_{gw})_i^j) = (1 - S_i^j)(\rho_{gw})_i^j + S_i^j (\rho_w)_i^j - X_i^j + Y_i^j$, where

$$\left[S((p_c)_i^j)\right]_i^j = \left[1 + \left(\frac{(p_c)_i^j}{p_b^c}\right)^n\right]^{-m}, \qquad \left[p_c((\rho_{gw})_i^j)\right]_i^j = -(\rho_w)_i^j \frac{R T_i^j}{M_w} \ln\left[\frac{T_i^j R}{(p^{gws})_i^j} (\rho_{gw})_i^j\right].$$

For given X_i^j, Y_i^j from (19) and (20), we find a solution $(\rho_{gw})_i^j$ of the nonlinear equation (21) written in the form

$$\mathcal{F}((\rho_{gw})_i^j) = 0, \tag{22}$$

with Newton's iteration procedure; the solution at the rst iteration is given by

$$\left\{(\rho_{gw})_i^j\right\}^r = \left\{(\rho_{gw})_i^j\right\}^{r-1} - \frac{\mathcal{F}'\left(\left\{(\rho_{gw})_i^j\right\}^{r-1}\right)}{\mathcal{F}\left(\left\{(\rho_{gw})_i^j\right\}^{r-1}\right)}, \tag{23}$$

where

$$\mathcal{F}'\left(\left\{(\rho_{gw})_i^j\right\}^{r-1}\right) = 1 - S\left(p_c\left((\rho_{gw})_i^j\right)\right) + \frac{\partial S}{\partial p_c} . p_c'\left((\rho_{gw})_i^j\right)\left((\rho_w)_i^j - (\rho_{gw})_i^j\right),$$

$$\frac{\partial S}{\partial p_c}(p_c) = -\frac{mn}{p_b^c}\left(\frac{p_c}{p_b^c}\right)^{n-1}\left[1 + \left(\frac{p_c}{p_b^c}\right)^n\right]^{-m-1}, \qquad p_c'(\rho_{gw}) = -\frac{T R \rho_w}{M_w \rho_{gw}}.$$

From boundary conditions (4) and (5) we get

$$\rho_{gw}(\mathbf{v}_g + \mathbf{v}_{gw}^d - \beta_c) + \rho_{ga}\mathbf{v}_{gw}^d = -\rho_w \mathbf{v}_l - \beta_c \rho_{gw\infty}, \tag{24}$$

$$p_{atm} = p_g = p_{ga} + p_{gw} = \frac{TR}{M_a}\rho_{ga} + \frac{TR}{M_w}\rho_{gw}, \tag{25}$$

where $\rho_{gw}(0)$ and $\rho_{ga}(0)$ are the solutions of (24) and (25) and finally

$$X_0^j = (1 - S_0^j)(\rho_{gw}(0) + \rho_{ga}(0)) + S_0^j(\rho_w)_0^j, \tag{26}$$

$$Y_0^j = (1 - S_0^j)\rho_{ga}(0). \tag{27}$$

Analogously, for the boundary conditions (6) and (7), we get

$$X_l^j = (1 - S_l^j)(\rho_{gw}(l) + \rho_{ga}(l)) + S_l^j(\rho_w)_l^j, \tag{28}$$

$$Y_l^j = (1 - S_l^j)\rho_{ga}(l). \tag{29}$$

5. Numerical results

Numerical algorithm was implemented in the model by coding in FORTRAN. Following figures show developments of temperature, saturation and water vapour pressure. An increase of temperature and capillary pressure and corresponding decrease of saturation are observed only in the confined layer in the range 50 mm from the heated surface. The swift evaporation of water inside the wall implies the rapid desaturation in the zone of increased vapour pressure. Analysis of these results allows for better understanding of hygro-thermal behaviour of concrete elements near the heated boundary.

6. Thermal spalling

In 1996 the fire with temperatures up to 700 °C occurred in the transport Tunnel connecting England and France, as in the similar case in 1999 in St. Gotthard tunnel,

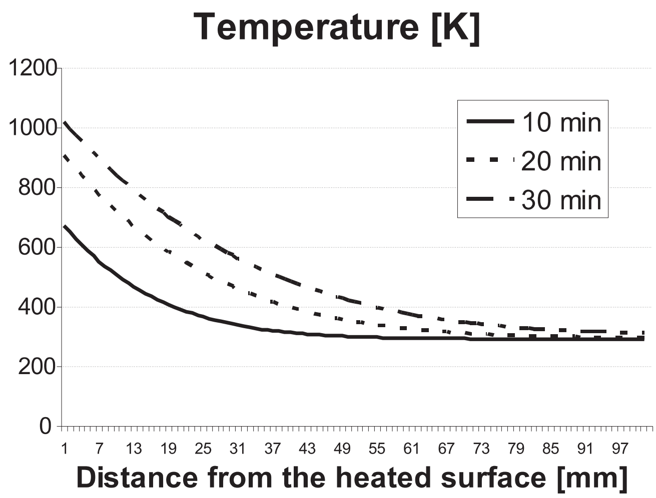

Fig. 1: *Temperature distributions.*

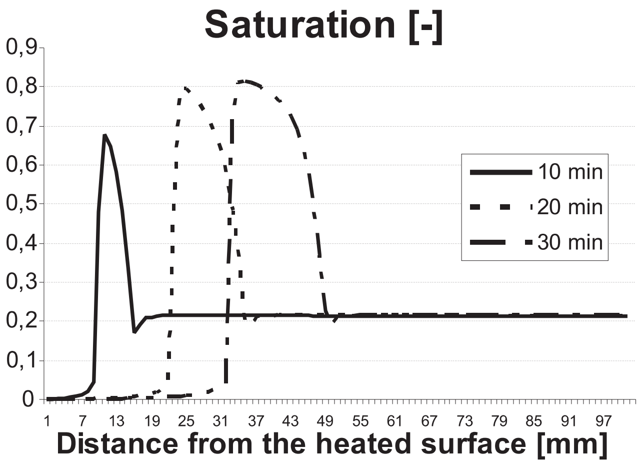

Fig. 2: *Saturation distributions.*

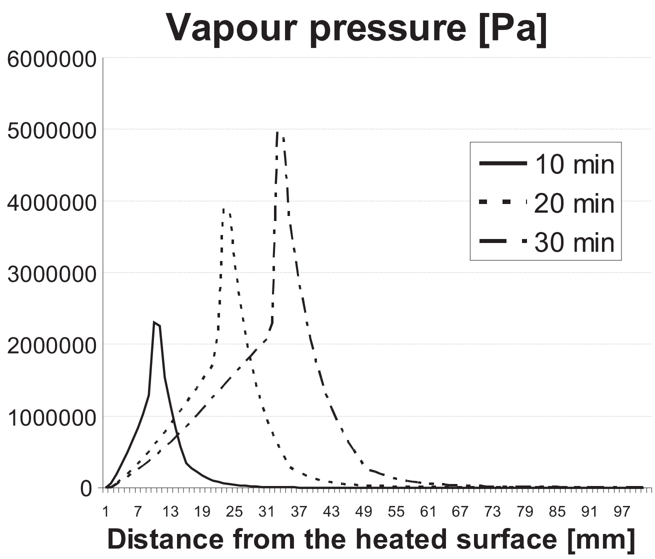

Fig. 3: *Vapour pressure distributions.*

the fire destroyed the concrete structure by thermal spalling over a length of a few hundred meters.

An interesting phenomenon, very specific for heated concrete, is the so-called thermal spalling, which can sometimes be explosive. Its physical causes are still not fully understood. Two main phenomena are generally considered to explain this transient thermal behavior of High Performance Concrete (see [4], [5], [6]):

- generation of internal vapor pressures, which exceed the local tensile strength of the material,
- thermo-mechanical stresses associated with thermal gradients increased by the local consumption of energy associated with vaporization and dehydration.

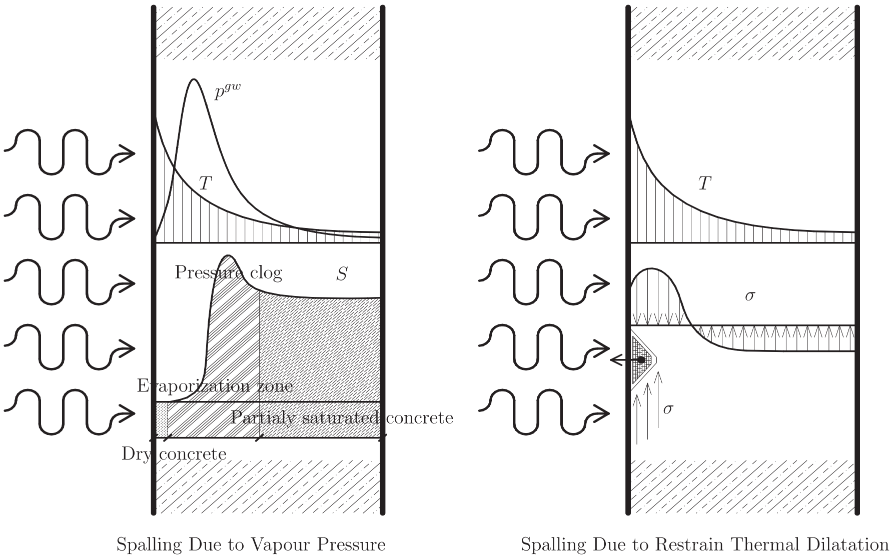

Fig. 4: *Thermal Spalling Hypothesis.*

References

[1] A.Y. Beliaev, S.M. Hassanizadeh: *A theoretical model of hysteresis and dynamic effects in the capillary relation for two-phase flow in porous media.* Transport in Porous Media **43**, 2001, 487–510.

[2] S.M. Hassanizadeh, W.G. Gray: *Mechanics and thermodynamics of multiphase flow in porous media including interphase boundaries.* Adv. Water Resour. **13**, 1990, 169–186.

[3] D. Gawin, C.-E. Majorana, B.-A. Schrefler: *Numerical analysis of hygro-thermal behaviour and damage of concrete at high temperature.* Mech. Cohes.-Frict. Mater. **4**, 1999, 37–74.

[4] D. Gawin, F. Pesavento, B.-A. Schrefler: *Towards prediction of the thermal spalling risk through a multi-phase porous media model of concrete.* Comput. Methods Appl. Mech. Engrg. **195**, 2006, 5707–5729.

[5] B.-A. Schrefler: *Multiphase flow in deforming porous material.* Int. J. Numer. Meth. Eng. **60**, 2004, 27–50.

[6] F.-J. Ulm, O. Coussy, Z.-P. Bažant: *The "Chunnel" fire. I: chemoplastic softening in rapidly heated concrete.* Journal of Engineering Mechanics **125**, 3, 1999, 283–289.